Journal of Achievements in Materials and Manufacturing Engineering
VOLUME 48
ISSUE 2
October
2011

Fe-based bulk metallic glasses prepared by centrifugal casting method

R. Nowosielski, R. Babilas*
Institute of Engineering Materials and Biomaterials, Silesian University of Technology, ul. Konarskiego 18a, 44-100 Gliwice, Poland
* Corresponding author: E-mail address: rafal.babilas@polsl.pl

Received 11.08.2011; published in revised form 01.10.2011

Materials

ABSTRACT

Purpose: The work presents a casting method, structure characterization and analysis of chosen properties of Fe-based bulk metallic glasses in as-cast state.
Design/methodology/approach: The studies were performed on $Fe_{72}B_{20}Si_4Nb_4$, $Fe_{36}Co_{36}B_{19}Si_5Nb_4$, $Fe_{43}Co_{14}Ni_{14}B_{20}Si_5Nb_4$ metallic glasses in form of rings. The amorphous structure of tested samples was examined by X-ray diffraction (XRD), transmission electron microscopy (TEM) and scanning electron microscopy (SEM) methods. The crystallization behaviour of the studied alloys was examined by differential thermal analysis (DTA). The soft magnetic property examinations of tested materials contained initial magnetic permeability and measurements of magnetic permeability relaxation.
Findings: The XRD and TEM investigations revealed that the studied as-cast bulk glassy samples in forms of ring were amorphous for all tested alloys. The SEM images showed that fractures of studied rings indicated two structurally different zones, which contained “river” patterns and “smooth” areas. The samples of studied alloys presented two stage crystallization process, which was observed for all tested rings with different thickness. The changes of crystallization temperatures versus the thickness of the glassy samples were stated. The magnetic permeability relaxation, which is directly proportional to the microvoids concentration in amorphous structure decreased with increase of sample thickness. These results could be assumed as the change of amorphous structure in function of thickness.
Practical implications: The centrifugal casting method is very simple, useful and effective method to produce bulk amorphous materials in the form of rings or tubes.
Originality/value: The preparation of bulk metallic glasses in the form of rings for three different Fe-based alloy systems is very important for the future progress in research and practical applications of iron-based bulk amorphous materials.
Keywords: Amorphous materials; Bulk metallic glasses; Thermal and magnetic properties; Centrifugal casting

Reference to this paper should be given in the following way:
R. Nowosielski, R. Babilas, Fe-based bulk metallic glasses prepared by centrifugal casting method, Journal of Achievements in Materials and Manufacturing Engineering 48/2 (2011) 153-160.

1. Introduction

The first metallic glasses were discovered over fifty years ago when rapid quenching methods were applied to solidification of liquid metal alloys. After that time, the significant development of many alloy systems with more improved glass-forming ability has been done [1,2].

The previous metallic glasses were generally fabricated by using cooling rate of 10^5 - 10^6 K/s. The more recently developed alloys required cooling rates of only 10^3 K/s or lower. Moreover, these alloy systems can be cast from the liquid state into glassy samples with thickness from several to one hundred millimetres. These alloys are called as 'bulk metallic glasses'. The recent development of bulk metallic glasses opened up new possibilities of investigations and applications for bulk metallic glasses [3,4].

The bulk amorphous alloys can be divided into nonferrous and ferrous types. It is important that bulk metallic glasses can be fabricated in specified engineering alloy systems such as Fe-, Co-, Ni-, Mg-, Ti-, Pd- and Zr-bases. The maximum glassy diameter of the bulk amorphous alloys tends to increase in the order of following elements: Pd > Zr > Ln = Mg > Fe > Ni > Co = Ti, which form main elements of alloy systems [5,6].

Inoue et al. succeeded in casting of Fe-based bulk metallic glasses in Fe-based alloy systems with low critical cooling rates below 10^3 K/s. Fe-based bulk metallic glasses with mentioned cooling rates have been often found in Fe-based alloy systems containing metalloids (B, C, Si and P) and early transition elements (Zr, Nb, Hf, Ta) [7].

The first Fe-based bulk glassy alloys were prepared in 1995, since then, a huge number of Fe-based bulk glassy alloys have been formed and their alloy components can be classified into five groups (Table 1). Fe-based bulk metallic glasses proposed by Inoue are represented by following systems: Fe-(Al,Ga)-(P,C,B,Si) Fe-(Zr,Hf,Nb,Ta)-B, Fe-(Cr,Mo)-(B-C), Fe-(Co,Ni)-B-Si-Nb and Fe-Nd-Al. It is important to know that Fe-based bulk metallic glasses with high strength of over 3300 MPa can be obtained only in two alloy groups of I and IV [8].

Table 1.
Classification of Fe-based bulk metallic glasses by Inoue [8]

Group	Fe-based alloy systems
I.	Fe-(Al,Ga)-(P,C,B,Si) Fe-(Cr,Mo,Nb)-(P,C,B,Si) Fe-Ga-(P,C,B,Si)
II.	Fe-(Zr,Hf,Nb,Ta)-B
III.	Fe-(Cr,Mo)-(C,B)
IV.	Fe-B-Si-Nb Fe-Co-B-Si-Nb
V.	Fe-Nd-Al

Iron-based metallic glasses have increased the scientific and engineering importance, because of their good soft magnetic properties, such as low coercive force, high magnetic induction and good magnetic permeability [9-14], mechanical properties [15-17] and formation of composite materials [18,19].

Many casting methods for fabrication of bulk metallic glasses have been developed. The main methods are described as copper mould casting, pressure die casting or suction casting [20-22].

Copper mould casting is the most common method to fabricate bulk metallic glasses in different alloy systems. In this method, the alloy is melted and put into copper mould where it is quickly solidified by rapid heat extraction of copper mould. Die casting is a useful method to preparation different types of castings for the industry applications. That method gives higher cooling rates in comparison with conventional casting techniques. The purpose of suction casting method is to inject the molten alloy into a mould by using a pressure differential between the melting chamber and the casting chamber [23].

More recently, Zhang et al. [24] had developed a centrifugal casting method to produce the Zr-based amorphous rings with a diameter of 25 mm and maximum thickness up to 2 mm. Moreover, Gao et al. [25] developed a centrifugal casting apparatus for a preparation of functionally graded materials.

Basing on literature [24,25] the paper presents using the conventional centrifugal casting method by rotating a copper based wheel to produced Fe-based amorphous rings.

2. Material and research methodology

The aim of the paper is presentation of the centrifugal casting method and investigations of microstructure, thermal and soft magnetic properties of Fe-based bulk metallic glasses in as-cast state. Investigations were done with use of XRD, TEM, SEM, DTA and magnetic measurements methods.

The investigated materials with the nominal composition of $Fe_{72}B_{20}Si_4Nb_4$, $Fe_{36}Co_{36}B_{19}Si_5Nb_4$, $Fe_{43}Co_{14}Ni_{14}B_{20}Si_5Nb_4$ were cast in form of the rings. The ingots of master alloys were prepared by induction melting of a mixture of pure elements under protective gas atmosphere.

The centrifugal casting method has been used to fabricate the ring samples of bulk metallic glass (Fig. 1) [26,27].

Figure 2 presents some photographs of a casting equipment (induction generator and casting apparatus "CentriCast"), which is applied to produced bulk metallic glasses by centrifugal casting method. The investigated bulk metallic glasses were cast in form of the ring with diameter of 30 mm and of different thickness. For alloy with composition of $Fe_{72}B_{20}Si_4Nb_4$ the samples had a thickness of 0.40 and 0.60 mm, the second metallic glasses $Fe_{36}Co_{36}B_{19}Si_5Nb_4$ were cast in form of rings with thickness of 0.30 and 0.40 mm and samples of $Fe_{43}Co_{14}Ni_{14}B_{20}Si_5Nb_4$ metallic glass were cast with thickness of 0.40 and 0.65 mm.

Structure analysis of the samples in as-cast state was carried out using X-ray diffractometer (XRD) with $Co_{K\alpha}$ radiation. The data of diffraction lines were recorded in 2θ range from 35° to 80° for samples of each alloy.

Transmission electron microscopy (TEM) was used for the structural characterization of rings in as-cast state. Thin foils for TEM observation (from central part of tested samples) were prepared by an electrolytic polishing method. The fracture morphology of the samples in form of ring was analysed using the scanning electron microscopy (SEM).

The thermal properties associated with onset (T_x) and peak (T_p) crystallization temperatures (for first and second stage) were measured using the differential thermal analysis (DTA) at a constant heating rate of 6 K/min under an argon protective atmosphere. DTA analysis was also used to define melting (T_m) and liquidus (T_l) temperature of master alloys.

Magnetic measurements of studied samples carried at room temperature included following properties [28-31]:

a) relative magnetic permeability (μ_r) - determined with Maxwell-Wien bridge at a frequency of 1030 Hz and magnetic field $H = 0.5$ A/m;
b) magnetic permeability relaxation ($\Delta\mu/\mu$) also defined as "magnetic after-effects" - determined by measuring changes of magnetic permeability as a function of time after demagnetization, where $\Delta\mu$ is difference between magnetic permeability determined at $t_1 = 30$ s and $t_2 = 1800$ s.

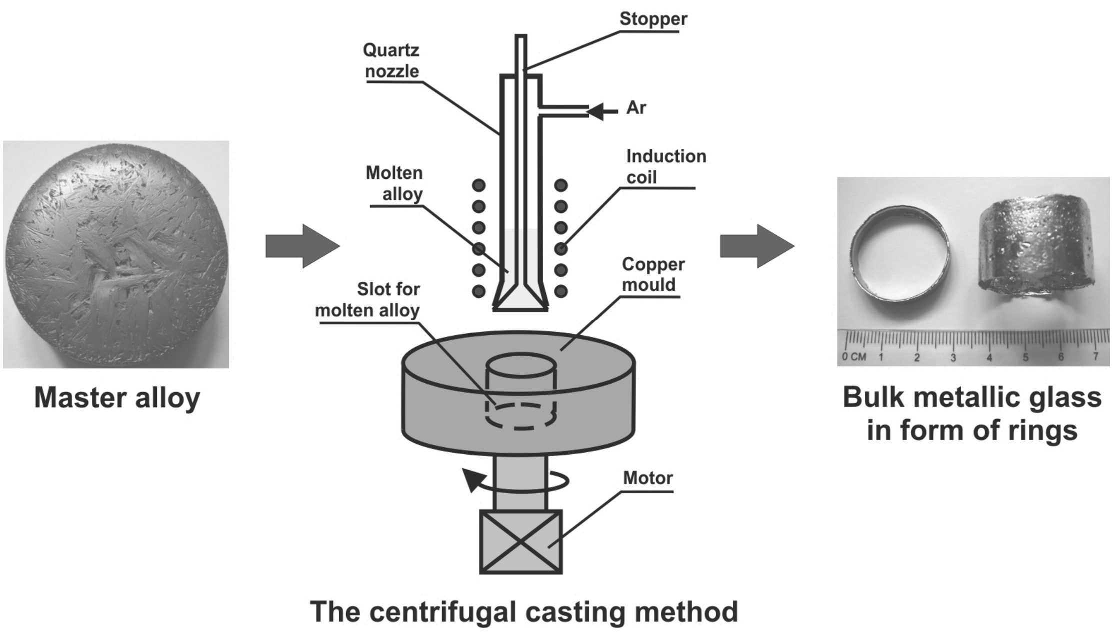

Fig. 1. Schematic illustration of the centrifugal casting method used for the casting of amorphous rings

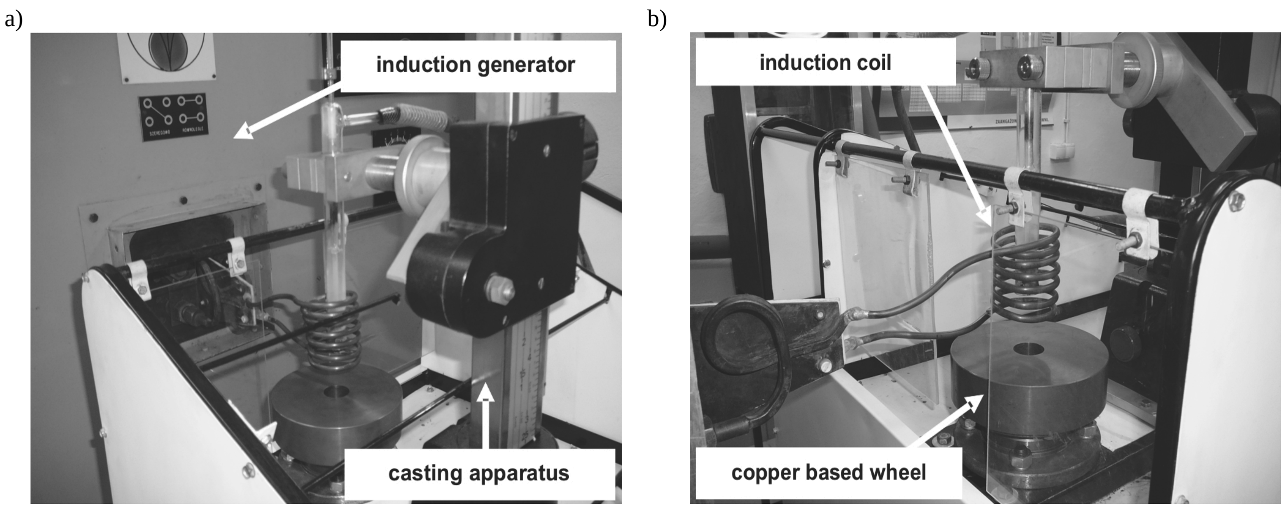

Fig. 2. The centrifugal casting equipment used for fabrication of bulk metallic glasses in form of rings: a) view of induction generator and casting apparatus "CentriCast", b) view of copper based wheel with casting slot

3. Results and discussion

The XRD investigations confirmed that the studied as-cast glassy samples were amorphous. The diffraction patterns of tested rings with constant diameter of 30 mm and thickness of 0.40 and 0.60 mm for $Fe_{72}B_{20}Si_4Nb_4$ metallic glass (Fig. 3), rings with thickness of 0.30 and 0.40 mm for $Fe_{36}Co_{36}B_{19}Si_5Nb_4$ alloy (Fig. 4) and samples with thickness of 0.40 and 0.65 mm for $Fe_{43}Co_{14}Ni_{14}B_{20}Si_5Nb_4$ alloy (Fig. 5) show in each case the broad diffraction halo.

This effect is typical for metallic amorphous materials, which have a structure with a large degree of short-range order of atoms.

Figures 6, 7 and 8 show TEM images and electron diffraction patterns of studied samples for each alloys in as-cast state. The TEM images reveal only a characteristic contrast for amorphous structure. The electron diffraction patterns consist only halo rings. Broad diffraction halo can be seen for each studied samples of all alloys and it also indicated the formation of a single glassy phase.

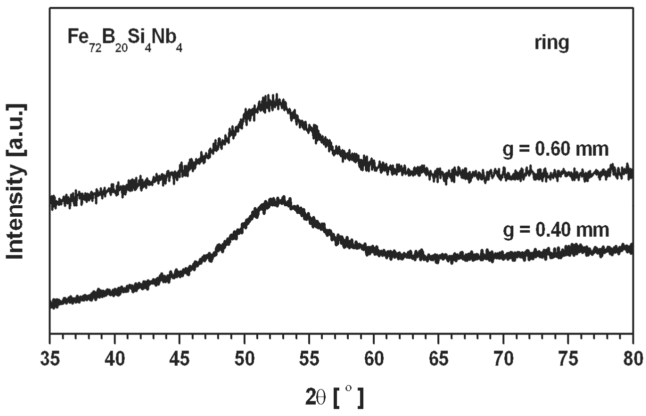

Fig. 3. X-ray diffraction patterns of $Fe_{72}B_{20}Si_4Nb_4$ glassy rings with diameter of 30 mm and thickness of 0.40 and 0.60 mm in as-cast state

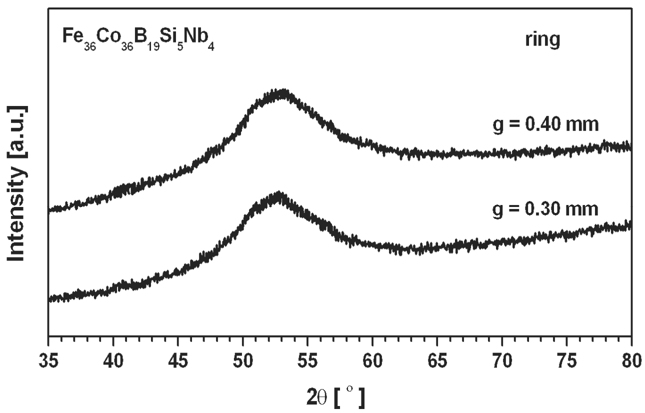

Fig. 4. X-ray diffraction patterns of $Fe_{36}Co_{36}B_{19}Si_5Nb_4$ glassy rings with diameter of 30 mm and thickness of 0.30 and 0.40 mm in as-cast state

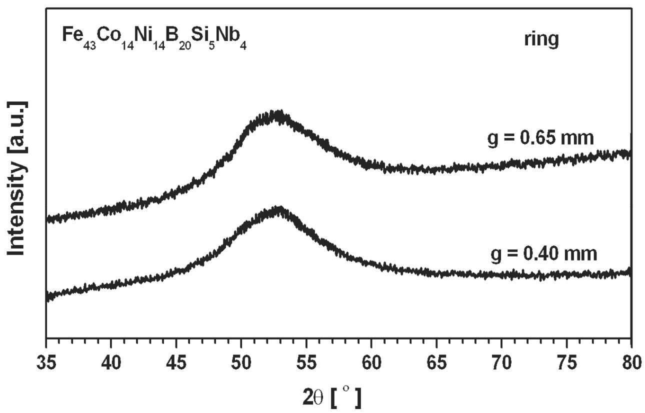

Fig. 5. X-ray diffraction patterns of $Fe_{43}Co_{14}Ni_{14}B_{20}Si_5Nb_4$ glassy rings with diameter of 30 mm and thickness of 0.40 and 0.65 mm in as-cast state

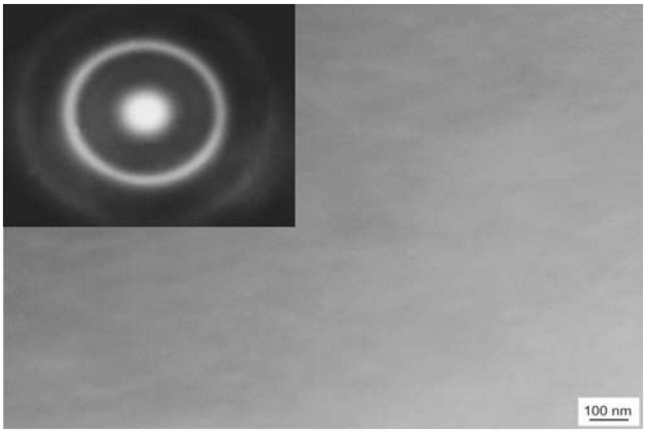

Fig. 6. Transmission electron micrograph plus electron diffraction pattern of $Fe_{72}B_{20}Si_4Nb_4$ glassy ring with thickness of 0.40 mm

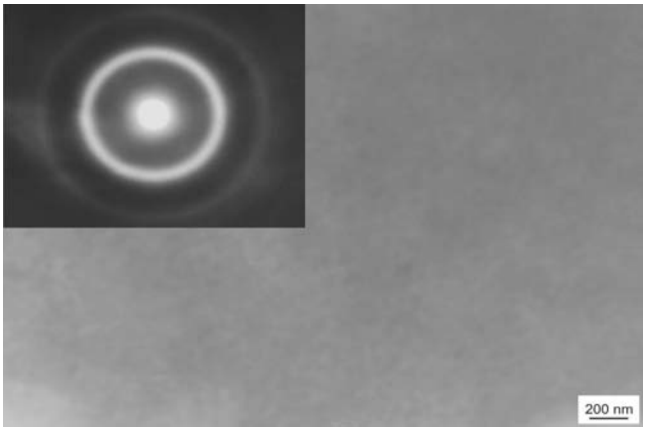

Fig. 7. Transmission electron micrograph plus electron diffraction pattern of $Fe_{36}Co_{36}B_{19}Si_5Nb_4$ glassy ring with thickness of 0.40 mm

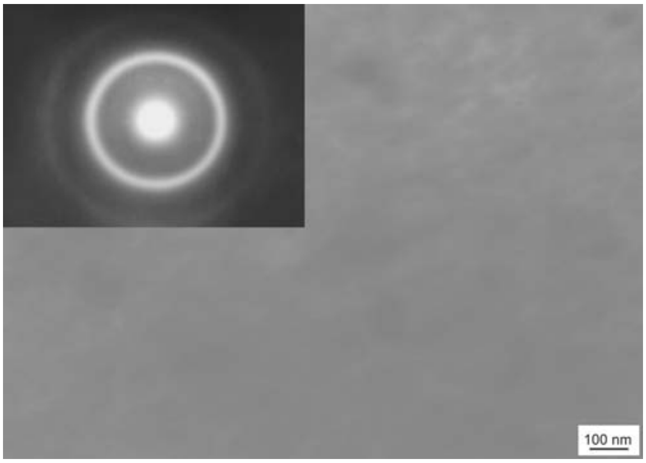

Fig. 8. Transmission electron micrograph plus electron diffraction pattern of $Fe_{43}Co_{14}Ni_{14}B_{20}Si_5Nb_4$ glassy ring with thickness of 0.65 mm

Results of DTA analysis (at 6 K/min) of master alloys of studied bulk metallic glasses are presented in Table 2, melting temperature (T_m) and liquidus temperature (T_l) are given.

The melting and liquidus temperature has a value of 1403 and 1433 K, adequately for master alloy of $Fe_{72}B_{20}Si_4Nb_4$ metallic glass. In the similar way, T_m has a value of 1313 K and T_l reached a value of 1363 K for $Fe_{36}Co_{36}B_{19}Si_5Nb_4$ alloy. Additionally, the melting temperature reached a value of 1318 K and liquidus temperature has a value of 1358 K for third studied alloy with composition of $Fe_{43}Co_{14}Ni_{14}B_{20}Si_5Nb_4$. The addition of Co and Ni into Fe-B-Si-Nb alloy has caused the decrease of melting and liquidus temperature of studied materials.

Table 2.
Thermal properties of $Fe_{72}B_{20}Si_4Nb_4$, $Fe_{36}Co_{36}B_{19}Si_5Nb_4$ and $Fe_{43}Co_{14}Ni_{14}B_{20}Si_5Nb_4$ master alloys

Master alloy	T_m, K	T_l, K
$Fe_{72}B_{20}Si_4Nb$	1403	1433
$Fe_{36}Co_{36}B_{19}Si_5Nb_4$	1313	1363
$Fe_{43}Co_{14}Ni_{14}B_{20}Si_5Nb_4$	1318	1358

The DTA curves (at 6 K/min) measured on amorphous rings with different thickness in as-cast state for studied alloy are shown in Figures 9, 10 and 11.

The two stage crystallization process was observed for all examined rings. The first stage crystallization of $Fe_{72}B_{20}Si_4Nb_4$ alloy for sample with thickness of 0.40 mm includes onset crystallization temperature (T_{x1} = 819 K) and peak crystallization temperature (T_{p1} = 845 K). The analysis of the second crystallization stage allows to determine only peak crystallization temperature (T_{p2}) with value of 922 K. Results of DTA analysis of ring with thickness of 0.60 mm also confirmed existing of T_{x1} = 820 K, T_{p1} = 844 K and T_{p2} = 921 K.

The first stage of crystallization obtained for samples of $Fe_{36}Co_{36}B_{19}Si_5Nb_4$ bulk metallic glass includes onset crystallization temperature at value of T_{x1} = 807 K for rings with thickness of 0.30 mm and 0.40 mm, similarly. The peak crystallization temperature has a value of T_{p1} = 833 K for ring with thickness of 0.30 mm and T_{p1} = 835 K for sample with thickness of 0.40 mm. The analysis of the second crystallization stage of studied samples allows to determine peak crystallization temperature, which has a value of 997 K (g = 0.30 mm) and 1000 K (g = 0.40 mm).

The DTA curves obtained for samples of $Fe_{43}Co_{14}Ni_{14}B_{20}Si_5Nb_4$ bulk metallic glass with thickness of 0.40 and 0.65 mm inform that the first stage of crystallization includes onset crystallization temperature at value of T_{x1} = 804 K. The peak crystallization temperature has a value of T_{p1} = 831 K for ring with thickness of 0.40 mm and 829 K for sample with thickness of 0.65 mm. The second crystallization stage of studied materials is described by peak with temperature of T_{p2} = 944 K for ring with thickness of 0.40 mm and temperature of T_{p2} = 942 K for sample with thickness of 0.65 mm.

The analysis of crystallization process of examined rings for three alloys shows that peak of crystallization temperature is changing with increasing of samples thickness. The differences of crystallization temperatures between rings with chosen thickness of the same alloy are probably caused by different amorphous structures as a result of the different cooling rates in casting process of studied bulk metallic glasses.

The thermal properties associated with onset (T_x) and peak (T_p) crystallization temperatures of studied glassy samples are presented in Table 3.

Table 3.
Thermal properties of the studied samples in forms of ring in as-cast state

Alloy	Thickness, mm	T_{x1}, K	T_{p1}, K	ΔT_{p2}, K
$Fe_{72}B_{20}Si_4Nb_4$	0.40	819	845	922
	0.60	820	844	921
$Fe_{36}Co_{36}B_{19}Si_5Nb_4$	0.30	807	833	997
	0.40	807	835	1000
$Fe_{43}Co_{14}Ni_{14}B_{20}Si_5Nb_4$	0.40	804	831	944
	0.65	804	829	942

The fracture surfaces of the investigated samples in form of rings were investigated by SEM at different magnifications. Figures 12, 13 and 14 present micrographs of selected areas of examined glassy materials.

The characteristic of the fracture surfaces showed different fracture zones. The fractures could be classified as mixed types with indicated two different kinds of zones. The first kind of fracture marked on the micrographs as “Zone I” contains weakly formed “river” and “shell” patterns and second one marked as “Zone II” contains “smooth” areas.

The investigated fracture surfaces of two different kinds of zones probably informed about different amorphous structures of the studied glassy rings for each alloy.

Finally, Table 4 presents information concerning some magnetic properties of the studied alloys in forms of the ring in as-cast state.

Generally, the initial magnetic permeability (μ_r) decreases with increasing of the thickness of studied rings. The μ_r obtained a value of 339 for sample of $Fe_{72}B_{20}Si_4Nb_4$ alloy with thickness of 0.40 mm and 176 for sample with thickness of 0.60 mm. Moreover, the initial magnetic permeability of $Fe_{36}Co_{36}B_{19}Si_5Nb_4$ bulk metallic glasses has a value of 424 for ring with thickness of 0.30 mm and μ_r = 212 for sample with thickness of 0.40 mm. Similarly, the μ_r has a value of 462 and 241 for rings of $Fe_{43}Co_{14}Ni_{14}B_{20}Si_5Nb_4$ alloy with thickness of 0.40 and 0.65 mm, adequately.

Basing on the works [28-31], the intensity of magnetic permeability relaxation ($\Delta\mu/\mu$) is directly proportional to the concentration of the defects in amorphous materials, i.e. free volume concentration. The value of the $\Delta\mu/\mu$ also decreases with increasing sample thickness for each studied alloy.

The magnetic permeability relaxation determined for samples in form of ring with thickness of 0.40 and 0.60 mm for $Fe_{72}B_{20}Si_4Nb_4$ alloy has a value of 5.9 and 3.7 %, accordingly.

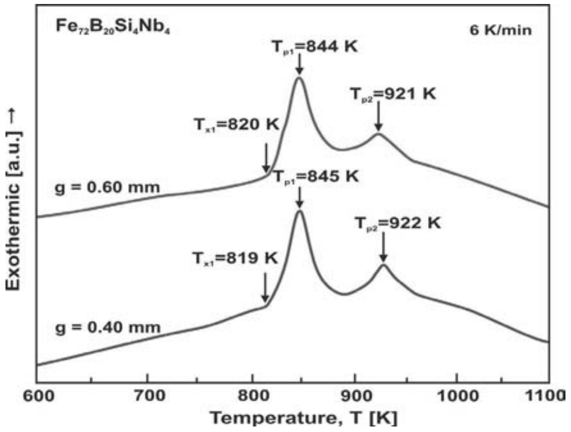

Fig. 9. DTA curves of $Fe_{72}B_{20}Si_4Nb_4$ glassy rings in as-cast state (heating rate 6 K/min)

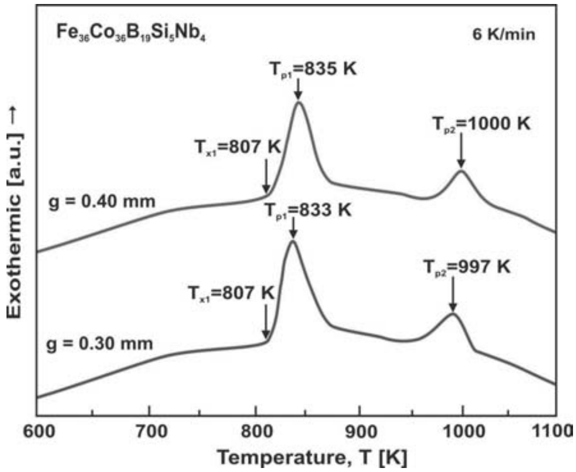

Fig. 10. DTA curves of $Fe_{36}Co_{36}B_{19}Si_5Nb_4$ glassy rings in as-cast state (heating rate 6 K/min)

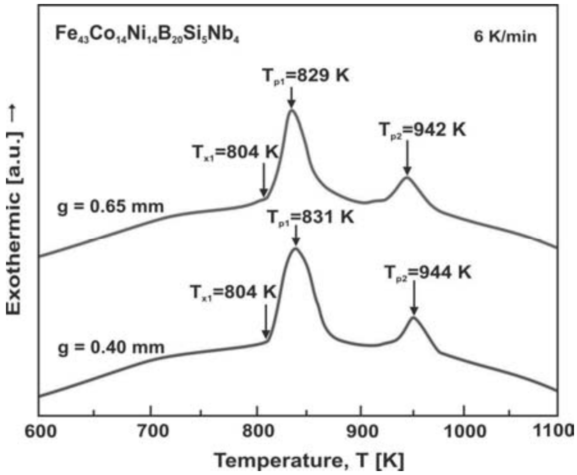

Fig. 11. DTA curves of $Fe_{43}Co_{14}Ni_{14}B_{20}Si_5Nb_4$ glassy rings in as-cast state (heating rate 6 K/min)

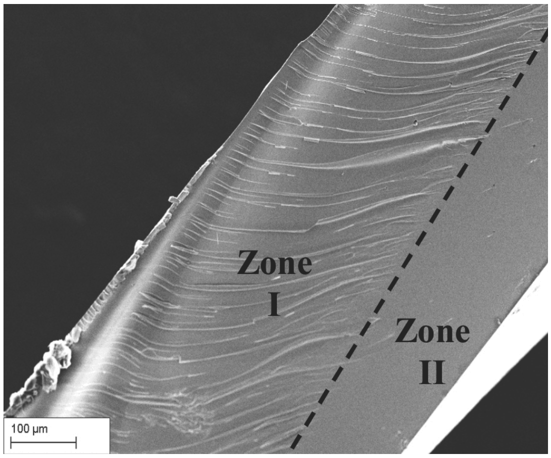

Fig. 12. Fracture morphology of $Fe_{72}B_{20}Si_4Nb_4$ glassy ring with diameter of 30 mm and thickness of 0.40 mm

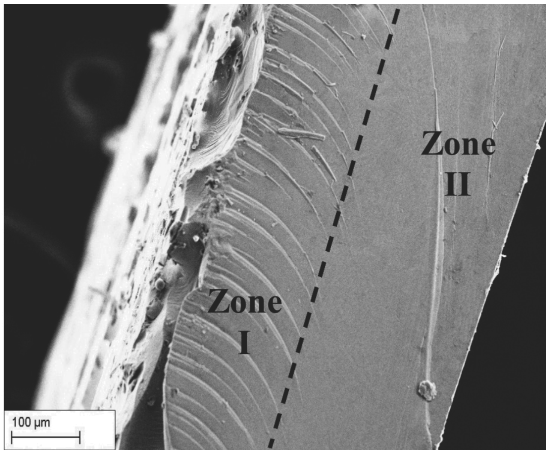

Fig. 13. Fracture morphology of $Fe_{36}Co_{36}B_{19}Si_5Nb_4$ glassy ring with diameter of 30 mm and thickness of 0.40 mm

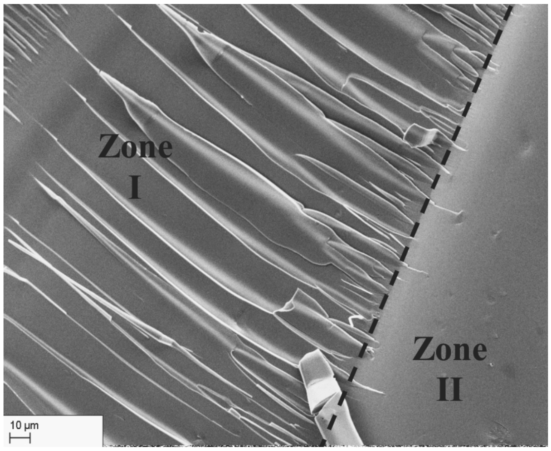

Fig. 14. Fracture morphology of $Fe_{43}Co_{14}Ni_{14}B_{20}Si_5Nb_4$ glassy ring with diameter of 30 mm and thickness of 0.40 m

Table 4.
Magnetic properties of the studied glassy alloys in forms of ring in as-cast state

Alloy	Thickness, mm	μ_r	$\Delta\mu/\mu$, %
$Fe_{72}B_{20}Si_4Nb_4$	0.40	339	5.9
	0.60	176	3.7
$Fe_{36}Co_{36}B_{19}Si_5Nb_4$	0.30	424	5.3
	0.40	212	5.0
$Fe_{43}Co_{14}Ni_{14}B_{20}Si_5Nb_4$	0.40	462	6.7
	0.65	241	2.7

For samples of second alloy ($Fe_{36}Co_{36}B_{19}Si_5Nb_4$) the $\Delta\mu/\mu$ has a value of 5.3 and 5.0% for rings with thickness of 0.30 and 0.40 mm. The magnetic permeability relaxation of studied rings of $Fe_{43}Co_{14}Ni_{14}B_{20}Si_5Nb_4$ alloy has a value of 6.7% for sample with thickness of 0.40 mm and the $\Delta\mu/\mu$ = 2.7% for sample with thickness of 0.65 mm.

4. Conclusions

The investigations performed on the studied bulk metallic glasses in form of rings allowed to formulate the following statements:

- The XRD and TEM investigations revealed that the studied as-cast bulk glassy samples in forms of ring were amorphous for all tested alloys,
- The liquidus temperature reached a value of 1433, 1363 and 1358 K for $Fe_{72}B_{20}Si_4Nb_4$, $Fe_{36}Co_{36}B_{19}Si_5Nb_4$ and $Fe_{43}Co_{14}Ni_{14}B_{20}Si_5Nb_4$ master alloy, adequately,
- The samples of studied alloys presented two stage crystallization process, which was observed for all tested rings with different thickness,
- Changes of crystallization temperatures versus the thickness of the glassy samples were stated,
- The SEM images showed that fractures of studied rings in as-cast state indicated two structurally different zones, which contain “river” patterns and “smooth” areas,
- The initial magnetic permeability determined for all studied glassy rings decreased with increasing of sample thickness,
- The magnetic permeability relaxation, which is directly proportional to the microvoids concentration in amorphous structure decreased with increasing of sample thickness and could be assumed as changing of amorphous structure in function of metallic glass thickness.

Acknowledgements

The authors would like to thank Dr A. Zajączkowski, Dr W. Głuchowski, (Non-Ferrous Metals Institute, Gliwice) and Dr Z. Stokłosa (Institute of Materials Science, University of Silesia, Katowice) for a cooperation.

References

[1] H.S. Chen, Glassy metals, Reports on Progress in Physics 43 (1980) 353-432.
[2] A. Inoue, K. Hashimoto, Amorphous and nanocrystalline materials: preparation, properties and applications, Springer, 2001.
[3] W.H. Wang, C. Dong, C.H. Shek, Bulk metallic glasses, Materials Science and Engineering R 44 (2004) 45-89.
[4] J. Basu, S. Ranganathan, Bulk metallic glasses: A new class of engineering materials, Sadhana 28 (2003) 783-798.
[5] A. Inoue, A. Takeuchi, T. Zhang, Ferromagnetic bulk amorphous alloys, Metallurgical and Materials Transactions A 29 (1998) 1779-1793.
[6] A. Inoue, A. Makino, T. Mizushima, Ferromagnetic bulk glassy alloys, Journal of Magnetism and Magnetic Materials 215-216 (2000) 246-252.
[7] A. Inoue, Bulk amorphous and nanocrystalline alloys with high functional properties, Materials Science and Engineering A 304-306 (2001) 1-10.
[8] A. Inoue, B.L. Shen, C.T. Chang, Fe- and Co-based bulk glassy alloys with ultrahigh strength of over 4000 MPa, Intermetallics 14 (2006) 936-944.
[9] L.A. Dobrzański, M. Drak, B. Ziębowicz, Materials with specific magnetic properties, Journal of Achievements in Materials and Manufacturing Engineering 17 (2006) 37-40.
[10] S. Lesz, D. Szewieczek, J.E. Frąckowiak, Structure and magnetic properties of amorphous and nanocrystalline $Fe_{85.4}Hf_{1.4}B_{13.2}$ alloy, Journal of Achievements in Materials and Manufacturing Engineering 19/1 (2006) 29-34.
[11] D. Szewieczek, T. Raszka, J. Olszewski, Optimisation the magnetic properties of the $(Fe_{1-x}Co_x)_{73.5}Cu_1Nb_3Si_{13.5}B_9$ (x=10; 30; 40) alloys, Journal of Achievements in Materials and Manufacturing Engineering 20 (2007) 31-36.
[12] D. Szewieczek, T. Raszka, Structure and magnetic properties of $Fe_{63.5}Co_{10}Cu_1Nb_3Si_{13.5}B_9$ alloy, Journal of Achievements in Materials and Manufacturing Engineering 19/2 (2006) 179-182.
[13] J. Konieczny, L.A. Dobrzański, A. Przybył, J.J. Wysłocki, Structure and magnetic properties of powder soft magnetic materials, Journal of Achievements in Materials and Manufacturing Engineering 20 (2007) 139-142.
[14] D. Szewieczek, T. Raszka, Influence of Na_2SO_4 on magnetic properties of $(Fe_{1-x})_{73.5}Cu_1Nb_3Si_{13.5}B_9$ (x = 10,40) alloys, Journal of Achievements in Materials and Manufacturing Engineering 17 (2006) 161-164.
[15] J. Konieczny, L.A. Dobrzański, J.E. Frąckowiak, Structure and properties of the powder obtained from the amorphous ribbon, Journal of Achievements in Materials and Manufacturing Engineering 18 (2006) 143-146.
[16] D. Szewieczek, J. Tyrlik-Held, S. Lesz, Structure and mechanical properties of amorphous $Fe_{84}Nb_7B_9$ alloy during crystallization, Journal of Achievements in Materials and Manufacturing Engineering 24/1 (2007) 87-90.
[17] S. Lesz, D. Szewieczek, J. Tyrlik-Held, Correlation between fracture morphology and mechanical properties of NANOPERM alloys, Archives of Materials Science and Engineering 29/2 (2008) 73-80.

[18] B. Ziębowicz, D. Szewieczek, L.A. Dobrzański, New possibilities of application of composite materials with soft magnetic properties, Journal of Achievements in Materials and Manufacturing Engineering 20 (2007) 207-210.

[19] L.A. Dobrzański, M. Drak, Hard magnetic composite materials Nd-Fe-B with additions of iron and X2CrNiMo-17-12-2 steel, Journal of Alloys and Compounds 449 (2008) 88-92.

[20] S. Lesz, Preparation of Fe-Co-based bulk amorphous alloy from high purity and industrial raw materials, Archives of Materials Science and Engineering 48/2 (2011) 77-88.

[21] R. Babilas, R. Nowosielski, Iron-based bulk amorphous alloys, Archives of Materials Science and Engineering 44/1 (2010) 5-27.

[22] R. Nowosielski, R. Babilas, S. Griner, Z. Stokłosa, Structure and soft magnetic properties of $Fe_{72}B_{20}Si_{4}Nb_{4}$ bulk metallic glasses, Archives of Materials Science and Engineering 35/1 (2009) 13-20.

[23] C. Suryanarayana, A. Inoue, Bulk metallic glasses, CRC Press, 2011.

[24] Q.S. Zhang, D.Y. Guo, A.M. Wang, H.F. Zhang, B.Z. Ding, Z.Q. Hu, Preparation of bulk $Zr_{55}Al_{10}Ni_{5}Cu_{30}$ metallic glass ring by centrifugal casting method, Intermetallics 10 (2002) 1197-1201.

[25] J.W. Gao, C.Y. Wang, Modeling the solidification of functionally graded materials by centrifugal casting, Materials Science and Engineering A 292 (2000) 207-215.

[26] R. Nowosielski, R. Babilas, Preparation, structure and properties of Fe-based bulk metallic glasses, Journal of Achievements in Materials and Manufacturing Engineering 40/2 (2010) 123-130.

[27] R. Nowosielski, R. Babilas, Fabrication of bulk metallic glasses by centrifugal casting method, Journal of Achievements in Materials and Manufacturing Engineering 20 (2007) 487-490.

[28] Z. Stokłosa, J. Rasek, P. Kwapuliński, G. Haneczok, G. Badura, J. Lelątko, Nanocrystallisation of amorphous alloys based on iron, Materials Science and Engineering C 23 (2003) 49-53.

[29] Z. Stokłosa, G. Badura, P. Kwapuliński, J. Rasek, G. Haneczok, J. Lelątko, L. Pająk, Influence of alloying additions on enhancement of soft magnetic properties effect and crystallisation in FeXSiB (X = Cu, V, Co, Zr, Nb) amorphous alloys, Solid State Phenomena 130 (2007) 171-174.

[30] P. Kwapuliński, J. Rasek, Z. Stokłosa, G. Badura, B. Kostrubiec, G. Haneczok, Magnetic and mechanical properties in FeXSiB (X=Cu, Zr, Co) amorphous alloys, Archives of Materials Science and Engineering 31/1 (2008) 25-28.

[31] P. Kwapuliński, Z. Stokłosa, J. Rasek, G. Badura, G. Haneczok, L. Pająk, L. Lelątko, Influence of alloying additions and annealing time on magnetic properties in amorphous alloys based on iron, Journal of Magnetism and Magnetic Materials 320 (2008) 778-782.